Local magnetism and spin dynamics of the frustrated honeycomb rhodate Li$_2$RhO$_3$

P. Khuntia,[1,*] S. Manni,[2,†] F. R. Foronda,[3] T. Lancaster,[4] S. J. Blundell,[3] P. Gegenwart,[2] and M. Baenitz[1,‡]

[1]*Max Planck Institute for Chemical Physics of Solids, 01187 Dresden, Germany*

[2]*EP VI, Center for Electronic Correlations and Magnetism, Augsburg University, D-86159 Augsburg, Germany*

[3]*Oxford University, Department of Physics, Clarendon Laboratory, Parks Road, Oxford OX1 3PU, United Kingdom*

[4]*Durham University, Centre for Materials Physics, Department of Physics, South Road, Durham DH1 3LE, United Kingdom*

We report magnetization, heat capacity, ^{7}Li nuclear magnetic resonance (NMR), and muon-spin rotation (μSR) measurements on the honeycomb $4d^5$ spin liquid candidate Li$_2$RhO$_3$. The magnetization in small magnetic fields provides evidence of the partial spin-freezing of a small fraction of Rh^{4+} moments at 6 K, whereas the Curie-Weiss behavior above 100 K suggests a pseudo-spin-1/2 paramagnet with a moment of about $2.2\mu_B$. The magnetic specific heat (C_m) exhibits no field dependence and demonstrates the absence of long-range magnetic order down to 0.35 K. C_m/T passes through a broad maximum at about 10 K and $C_m \propto T^2$ at low temperatures. Measurements of the spin-lattice relaxation rate ($1/T_1$) reveal a gapless slowing-down of spin fluctuations upon cooling with $1/T_1 \sim T^{2.2}$. The results from NMR and μSR are consistent with a scenario in which a minority of Rh^{4+} moments are in a short-range correlated frozen state and coexist with a majority of moments in a liquid-like state that continue to fluctuate at low temperatures.

I. INTRODUCTION

The physics of $S = \frac{1}{2}$ quantum magnets (QMs) is extremely rich, owing to the variety of magnetic exchange interaction networks in different systems, as determined by the lattice geometry and the orbital hybridization [1,2]. Systems studied so far include quasi-one-dimensional (1D) linear chains, planar 2D systems (ladders, kagome layers, triangles, or square lattices), and more complex 3D structures such as hyperkagome and pyrochlore lattices. Recently, the field of $S = \frac{1}{2}$ quantum magnetism has been extended away from $3d$ ions (such as those containing Cu^{2+} or V^{4+} ions) towards $4d$ and $5d$ systems [1]. In these materials an effective $j_{\text{eff}} = \frac{1}{2}$ moment can be realized due to strong spin-orbit coupling (SOC), and in certain compounds the presence of frustration is suspected to lead to a quantum spin-liquid (QSL) ground state [3]. In general, having the energy of the SOC, the Coulomb interaction (parametrized by U) and the crystal electric-field splitting of the same order of magnitude lead to highly degenerate magnetic states and complex excitations for many $4d$ and $5d$ QMs. These excitations can be gapless or gapped, but their nature is complicated by the presence of disorder and anisotropic interactions, and their understanding is hindered by the scarcity of model materials [1,3]. One approach to describing the highly degenerate states in such frustrated systems utilizes a fermionic bandlike picture with chargeless spinon ($S = \frac{1}{2}$) excitations. The fermionic spinon concept was first introduced in cuprates [4] and for organic Cu-based QSLs [5,6]. It was later established in other QMs, such as spin chains [7], 2D systems [8–10], and 3D networks including pyrochlore lattices [11,12].

Honeycomb $4d$ and $5d$ planar QMs have become attractive systems to study following the discovery of graphene, a honeycomb 2D Dirac semimetal; its unique properties stem from its linear dispersive modes ($E \sim k$) and its T-linear density of states at the Fermi level $N(E_F)$ [13]. These properties lead to T^2 behavior of the electronic specific heat [$\propto T N(E_F)$] and a T^3 power law for the spin-lattice relaxation rate $1/T_1$ [$\propto T N^2(E_F)$] [13,14]. By analogy, 2D honeycomb QSLs, with linear dispersive fermionic spinon bands and low-energy gapless magnetic excitations (spinons or Majorana fermions), are expected to exhibit T^2 behavior of the magnetic specific heat [15–17] and also power-law spin-lattice relaxation: $1/T_1 \sim T^n$ [15–20].

The theoretically solvable Heisenberg-Kitaev model [21–24] predicts that a honeycomb lattice decorated with $j_{\text{eff}} = \frac{1}{2}$ pseudospins can have a QSL ground state. Experimental realizations of this include (Li,Na)$_2$IrO$_3$ and α-RuCl$_3$ [25–36]. Na$_2$IrO$_3$ displays zigzag magnetic ordering, while α-Li$_2$IrO$_3$ exhibits incommensurate spiral ordering. α-RuCl$_3$ exhibits a complex magnetic ordered state, while recent NMR results suggest a gapping-out of magnetic excitations towards low temperatures once the order is suppressed by a magnetic field [27,32]. Surprisingly, the structural $4d$ homologue Li$_2$RhO$_3$ also shows insulating behavior in spite of reduced spin-orbit interactions [37], and even more interestingly this system exhibits no sign of long-range magnetic ordering (LRO), unlike its Ir counterpart [38]. Magnetic exchange between Rh^{4+} ions are expected to be highly frustrated, which makes this pseudospin $j_{\text{eff}} = \frac{1}{2}$ system a promising candidate for a Kitaev QSL. Here we provide a comprehensive account of the local magnetic properties of Li$_2$RhO$_3$ probed by ^{7}Li ($I = 3/2$) NMR and muon-spin rotation (μSR) accompanied by magnetization and heat capacity measurements down to 0.4 K.

II. RESULTS AND DISCUSSION

Polycrystalline samples of Li$_2$RhO$_3$ were synthesized by a method described elsewhere (see the Supplemental

---

*Present address: Department of Physics, Indian Institute of Technology, Madras Chennai 600036, India.

†Present address: Department of Physics and Astronomy, Iowa State University, Ames, Iowa 50011, USA.
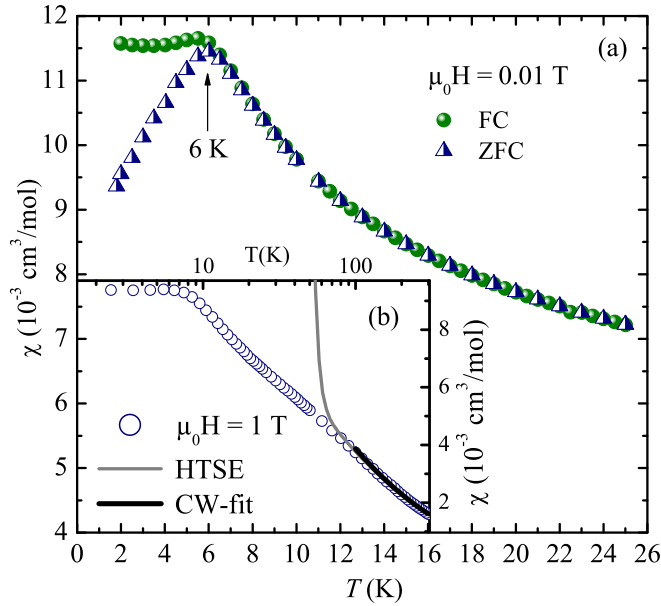
‡Corresponding author: baenitz@cpfs.mpg.de

FIG. 1. (a) Temperature dependence of the ZFC and FC susceptibility $\chi(T)$ measured in an applied field of 0.01 T. (b) $\chi(T)$ at 1 T, with HTSE (high-temperature series expansion) and CW (Curie-Weiss) fits as discussed in the text.

FIG. 2. (a) Magnetic heat capacity coefficient (C_m/T) in various fields as a function of $T/|\theta_{CW}|$. The upper axis shows the absolute T dependence and the solid line represents a T-linear fit, as discussed in the text. (b) T dependence of the magnetic entropy in zero field. (c) T dependence of the total heat capacity in zero field for Li$_2$RhO$_3$ compared with the nonmagnetic homologue Li$_2$SnO$_3$. The dashed line indicates T^2 behavior.

Material [39]). Shown in Fig. 1(a) is the temperature dependence of the dc magnetic susceptibility $\chi(T)$ measured following zero-field-cooled (ZFC) and field-cooled (FC) protocols at 10 mT. The ZFC and the FC $\chi(T)$ curves split at 6 K, which may arise from the short range ordering (SRO) due to partial freezing of Rh moments. However, the splitting in $\chi(T)$ is small, which indicates that probably only a small fraction of moments participates in the glassy state. SRO effects ("spin-freezing") admixed onto the QSL state have been discussed in quite a large number of materials, such as Na$_4$Ir$_3$O$_8$ and Ni$_2$Ga$_2$S$_4$ [41–50]. The Curie-Weiss (CW) fit [Fig. 1(b)] in the range $100 \leqslant T \leqslant 300$ K yields an effective moment of $2.2\mu_B$ per Rh ion. This is well above the spin-only value for the $S = \frac{1}{2}$ low-spin configuration of the $4d^5$ state of Rh^{4+}, which points towards moderate SOC [37,38,51]. The negative sign of the CW temperature, $\theta_{CW} = -60$ K, suggests the prominence of antiferromagnetic correlations between Rh^{4+} moments. The exchange interaction between the nearest-neighbor Rh^{4+} moments can be determined from the high-temperature series expansion, frequently used for honeycomb lattices with moderate SOC (such as $4d^5$ Ru^{3+} ions in α-RuCl$_3$). The high-temperature series expansion yields an antiferromagnetic interaction of $J/k_B \approx 75 \pm 5$ K and is in reasonable agreement with that obtained from the mean-field approximation [39,52]. The ac susceptibility exhibits a peak at about $T_g \approx 6$ K [39] and the peak positions are weakly frequency dependent, showing the role of dissipative spin dynamics in driving such a short-range spin-freezing mechanism. The origin of this partial spin-freezing might be related to the presence of local disorder in the lattice of Li$_2$RhO$_3$ [51,53–55] (see discussion in [39]) and the glassy feature smears out at higher fields ($\mu_0 H > 1$ T) [see Fig. 1(b)]. It may be noted that the spin-freezing effect
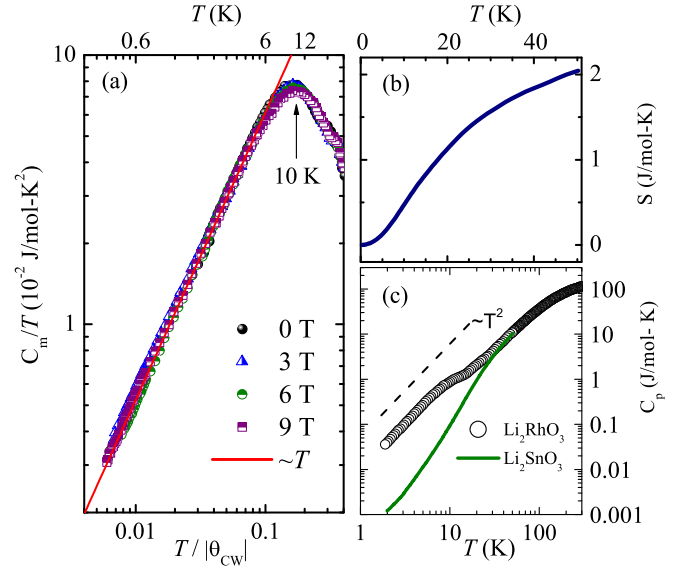
on the magnetization and the heat capacity in Li$_2$RhO$_3$ is rather minor in comparison with the textbook spin-glass materials [56].

The heat capacity coefficient C_m/T obtained in different magnetic fields is shown in Fig. 2(a). The heat capacity exhibits no signature of LRO down to 0.35 K. The magnetic heat capacity (C_m) was obtained by subtracting the lattice contribution using Li$_2$SnO$_3$ [see Fig. 2(c)] as a reference. As shown in Fig. 2(a), C_m/T displays a broad maximum at about 10 K, which could be associated with the highly frustrated nature of the system as discussed in spin liquids [1,45,57]. The strength of the exchange coupling and dimensionality of the system accounts for the position of the broad maximum in C_m and it varies as $T/|\theta_{CW}|$ in frustrated magnets. In Li$_2$RhO$_3$, we found $T/|\theta_{CW}| \approx 0.16$, which is comparable with those values in other $3d$ and $5d$ frustrated magnets [41,45,58]. The magnetic entropy $S_m = \int C_m/T \, dT$ up to 45 K was found to be only 35% [$\approx$2.04 J/mol K; Fig. 2(b)] of $R \ln 2$ ($\approx$5.76 J/mol K), consistent with the presence of short-range spin correlations. Below 10 K, C_m exhibits T^2 behavior [Fig. 2(a)], indicating the persistence of spin dynamics with low-lying gapless excitations, which is in agreement with the finite value of χ at low T in the context of the QSL state. The T^2 dependence of C_m is frequently found in $4d$ and $5d$ QMs as a fingerprint of the spin-liquid ground state [23,59,60].

The ^{7}Li NMR powder spectra at 70 MHz shown in Fig. 3(a) show a single Li NMR line which exhibits a clear broadening towards low temperatures without any strong anisotropy. The spectra consist of superimposed intensities from three powder-averaged Li lines from the three Li sites in the lattice structure (see Supplemental Material [39] for more details). The inset in Fig. 4(a) represents the T-dependent NMR shift, $K(T)$,
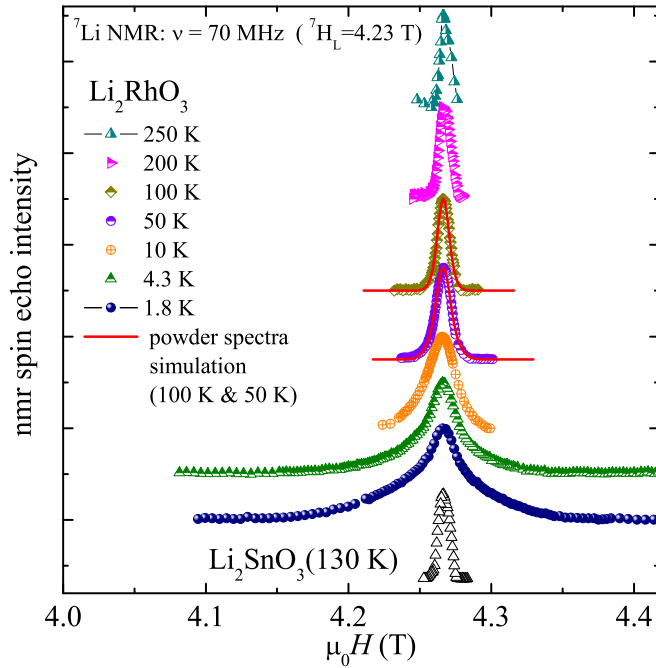
FIG. 3. Representative field-swept ^{7}Li-NMR spectra in Li$_2$RhO$_3$ at different temperatures (the solid line is a simulation for 100 K and for 50 K). At the bottom we show the ^{7}Li-NMR spectrum at 130 K for the nonmagnetic structural homologue Li$_2$SnO$_3$.

estimated from the simulation of each powder spectrum [see solid line in Fig. 3(a)]. The T dependence of the shift is reminiscent of the bulk susceptibility [Fig. 1(b)]. $K(T)$ consists of a T-dependent part, $K_{Rh}(T)$, due to the coupling of the Rh^{4+} moments with the Li nuclear spins and a nearly T-independent orbital part, K_{orb}, which is enhanced due to the presence of moderate spin-orbit interaction [60,61]. The linear scaling between K and χ (given by $K = A_{hf}\chi/N_A$) at high T yields
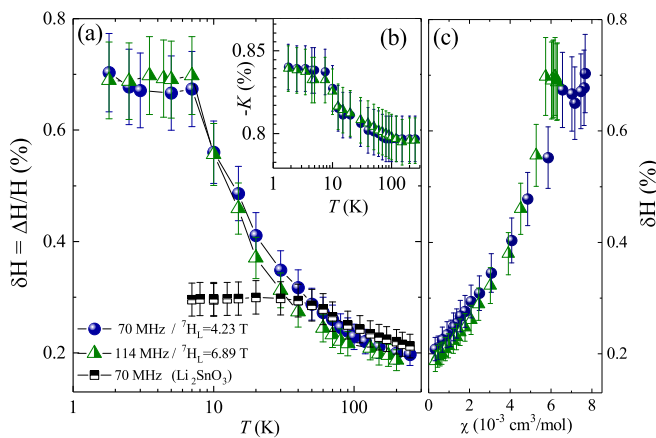

FIG. 4. (a) The T dependence of the full width at half-maximum (FWHM) line width divided by the resonance field (=relative line width; $\delta H = \Delta H/H$) at 70 and 114 MHz compared with $\delta(H)$ of the nonmagnetic homologue Li$_2$SnO$_3$. (b) T-dependent NMR shift, K, at 70 and 114 MHz. (c) $\delta H(T)$ vs $\chi(T)$ (obtained at the NMR fields) with T as an implicit parameter. The Larmor fields are calculated using the ^{7}Li gyromagnetic ratio of 16.5459 MHz/T.

a hyperfine coupling constant $A_{hf} = -(0.3 \pm 0.06)$ kOe/μ_B between the ^{7}Li nucleus and the Rh^{4+} electron spin. Figure 4(a) shows the NMR line width (FWHM) divided by the resonance field (therefore the relative line width, $\delta H = \Delta H/H$) at two NMR frequencies. The relative line width δH exhibits no field dependency and follows the bulk susceptibility [see Fig. 1(b)]. To account for the effect of the first-order quadrupolar splitting on the line broadening of the ^{7}Li NMR powder spectra we have investigated the nonmagnetic homologue Li$_2$SnO$_3$ under the same NMR conditions (see Supplemental Material [39]). This provides clear evidence that the low-temperature broadening is a generic feature of Li$_2$RhO$_3$ and the scaling with the bulk susceptibility demonstrates the magnetic origin of the broadening. The broadening is associated with static and slow fluctuating hyperfine field contributions at the nuclei sites. It is remarkable that δH is independent of the magnetic field. This implies that the absolute width is field dependent, suggesting that at these fields the system is not yet in the fully polarized state and sizable correlations among Rh^{4+} moments are still present. This is consistent with the absence of LRO in C_m down to 0.35 K. The saturation of $\delta H(T)$ at low T indicates the persistence of a quasistatic distribution of local magnetic fields and a slowing-down of magnetic fluctuations such that Rh^{4+} moments fluctuate at a frequency lower than the NMR frequency. The fact that above approximately 100 K (see Fig. 4(a) and Supplemental Material [39]) Li$_2$RhO$_3$ and Li$_2$SnO$_3$ have comparable NMR line widths suggests that the effect of antisite order (Li-Rh or Li-Sn) on the line width, discussed frequently in the literature [62], can be neglected (see discussion in [39]). The magnetic moment of 0.8μ_B estimated from the NMR line width at about 4 K and in an NMR field of 4.23 T (70 MHz) is small compared to the Rh^{4+} CW moment and suggests the presence of strong quantum fluctuations induced by magnetic frustration [43,63]. We found no loss of NMR signal intensity, typical for some disordered materials, which indicates that Li$_2$RhO$_3$ is not a conventional spin-glass material. This scenario is further supported by the absence of rectangular-shaped powder-averaged NMR spectra expected for materials that show LRO [64] and, moreover, by the field independence of the relative line width. The quasistatic NMR results presented so far support the scenario of a minority of moments in a short-range-like frozen state coexisting with the majority of moments, which remain liquid-like and which fluctuate at low T [41–45].

NMR spin-lattice relaxation rate measurements are very suitable for probing slow spin excitations because in general $1/T_1$ tracks the q-dependent complex dynamic spin susceptibility (see [39] for more details). Figure 5(a) shows $1/T_1$ vs T at two NMR frequencies (fields). Towards low temperatures $1/T_1$ decreases linearly with T and passes through a broad maximum around 10 K. This maximum could not be associated with conventional SG freezing, where a critical slowing-down of spin fluctuations at T_g leads to a very short T_1 and an NMR signal wipeout at low and intermediate T [43,63]. As shown in Fig. 5(a), $1/T_1$ decreases upon further cooling below 10 K and displays pronounced $T^{2.2}$ behavior down to 1.8 K. In principle, $1/T_1$ tracks the spectral density of the Fourier transform of the time correlation function of the transverse component δh_+ of the fluctuating local field at nuclear sites $h_{\pm}(0)$ with the nuclear Larmor frequency $\omega_N = \gamma H$
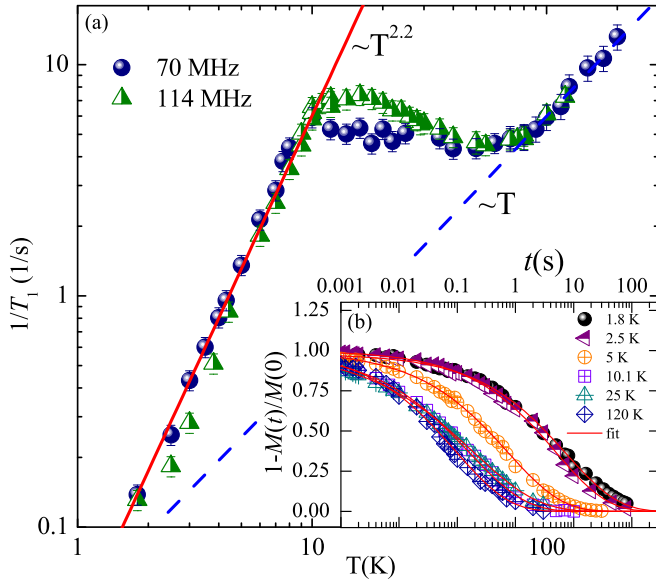
FIG. 5. (a) T dependence of $1/T_1$ at two NMR frequencies (fields). The solid line indicates a $T^{2.2}$ behavior below 10 K, whereas the dashed line depicts the T-linear behavior around 100 K. (b) Longitudinal magnetization recovery curves $M(t)$ at various temperatures in a semilog plot. Solid curves are the individual fits of the data with a stretched exponential function (see Supplemental Material [39] for more details) at various temperatures.

FIG. 6. (a) Representative μSR spectra for Li_2RhO_3 measured over a range of temperatures. (b) Fitted precession frequency ν_μ, which indicates the average field experienced by the muon in the spin frozen state (filled black circles; left axis), and relaxation rate λ of the slowly relaxing component (open red squares; right axis). (c) The amplitude A_f of the fast-relaxing component (filled black circles; left axis) and λ (open red squares; right axis).

as [65–67] $\frac{1}{T_1} = \frac{\gamma_N^2}{2} \int_{-\infty}^{+\infty} \langle h_\pm(t)h_\pm(0) \rangle e^{i\omega_N t} \, dt$, where γ_N is the gyromagnetic ratio of the nuclear spin. Assuming that the time correlation function varies as $e^{-\Gamma t}$, one can express $R = \frac{1}{T_1 T K} = A \frac{\Gamma}{\omega_c^2 + \omega_N^2}$, where A depends on the hyperfine coupling constant and K is the isotropic NMR shift. Here, ω_c corresponds to the fluctuation frequency of the fluctuating hyperfine field at the ^{7}Li nucleus site transferred from the fluctuating Rh^{4+} moments. One would expect $R \approx 1/\omega_c$ when $\omega_c \gg \omega_N$, while for $\omega_c \ll \omega_N$ one should find that R depends on the NMR field ($R \approx 1/\omega_N$). When $\omega_c = \omega_N$, $R(T)$ approaches a maximum (see Supplemental Material [39], Fig. S2), which is a consequence of the slowing-down of the fluctuation frequency ω_c of Rh^{4+} moments. We find that ω_c is nearly T independent at high T but decreases below 10 K as $\omega_c \propto T^{1.2}$ at low T, suggesting the slow spin dynamics of Rh^{4+}. This is consistent with the broad NMR line at low T. The slowing-down of spin fluctuations might then dominate the low-temperature magnetic properties [42,43]. The power-law dependence of $1/T_1$ can be compared with that found in the SOC-driven 5d spin-liquid compound $Na_4Ir_3O_8$ [47] and other low-dimensional QMs [18,19,63,68,69], which is attributed to the existence of a gapless state in the spin excitation spectrum and is in accord with the finite value of χ and K, and $C_m \sim T^2$ behavior at low T. The longitudinal nuclear spin-lattice relaxation rate is given by the low-energy (ω) and momentum-space (q) integrated hyperfine form factor $A(q,\omega)$ and the imaginary part of the complex dynamic electron susceptibility $\chi''(q,\omega)$ [proportional to $S(q,\omega)$, the dynamic structure factor]. For a 2D Kitaev spin liquid calculations of $S(q,\omega)$ suggest either gapped [$1/T_1 \sim \exp(-\Delta/k_B T)$] or gapless ($1/T_1 \sim T^n$) behavior [16,18,19]. For Li_2RhO_3, the

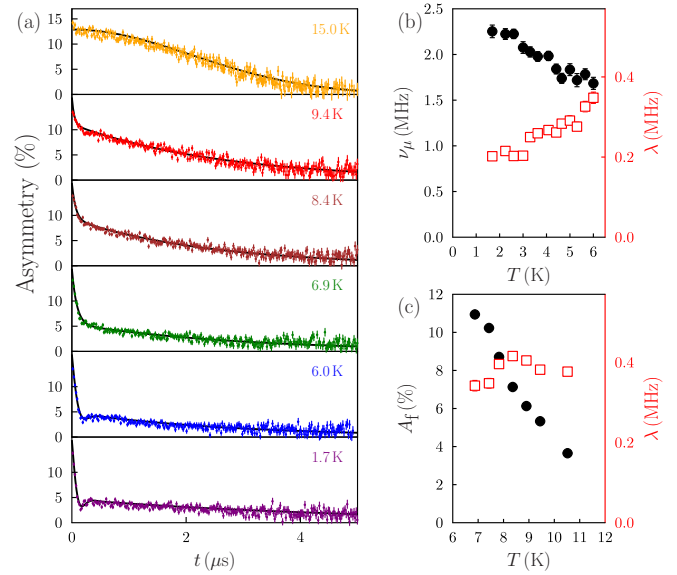gapless $T^{2.2}$ power law or, alternatively, the (pseudo-)gapped behavior [i.e., $1/T_1 \sim \exp(-\Delta/k_B T)$ + constant] reasonably fit the $1/T_1$ data (see Supplemental Material [39], Fig. S4).

Our μSR [70] experiments were carried out at Paul Scherrer Institut (PSI). Representative spectra are shown in Fig. 6(a). For temperatures below about 6 K, there is a single heavily damped oscillatory signal [proportional to $\cos(2\pi\nu_\mu t)e^{-\Delta t}$] together with a slow relaxation (proportional to $e^{-\lambda t}$). The damped oscillation signifies static magnetic Rh^{4+} moments but the large damping is entirely consistent with moment freezing and is not associated with long-range magnetic ordering. Fluctuations persist at low temperatures, evidenced by the presence of slow relaxation. The frequency of the damped oscillation, ν_μ, is around 2 MHz and falls slightly upon warming [see Fig. 6(b)], while the relaxation rate λ rises. At T above $\approx$6 K, it is no longer possible to fit the fast relaxation with a damped oscillation, and we identify this T with the freezing temperature T_g, in agreement with magnetization measurements [37,38] and coinciding with the peak measured in ac susceptibility (see Supplemental Material [39]). For $T > T_g$ we fit our data instead using the sum of two exponential relaxations, so that the fitting function becomes $A(t) = A(0)[A_f e^{-\Lambda t} + (1 - A_f)e^{-\lambda t}]$. The amplitude of the fast relaxing term A_f decreases upon warming above 6 K [see Fig. 6(c)] and is entirely absent by 15 K, by which temperature the relaxation is dominated by a Gaussian response characteristic of static nuclear moments. These observations indicate that although the freezing disappears above T_g there remain some frozen regions of the sample which persist well above T_g, up to almost 2T_g, perhaps in small, slowly fluctuating clusters. These slow fluctuations may likely contribute to the slow relaxation that is observed in these data.

The volume fraction of the clusters decreases upon warming and this can be directly related to the decrease in A_f. In fact, the observation of a slowly relaxing fraction throughout the temperature range demonstrates that the frozen state possesses some weak dynamics. These measurements are consistent with the development of a moment-frozen state below 6 K at small magnetic fields.

III. CONCLUSION

We have presented a study on the magnetism of Li_2RhO_3 to probe a possible spin-liquid ground state and investigate the presence of partial frozen moments. Whereas frozen moments were evidenced by low field susceptibility measurements, NMR measurements performed at a higher field could hardly resolve this effect. The zero-field μSR evidences frozen moments but also persistent low-energy spin dynamics. χ, δH, and K remain finite towards low T, whereas the magnetic specific heat as well as the spin lattice relaxation rate exhibits characteristic temperature dependencies assigned to quantum spin liquids. The magnetic heat capacity C_m displays no signature of LRO down to 0.35 K despite an antiferromagnetic interaction $J/k_B \approx 75$ K between Rh^{4+} moments. The $C_m \sim T^2$ and the $1/T_1 \sim T^{2.2}$ behavior at low T might be assigned to gapless excitations as predicted for the Kitaev quantum spin-liquid state. Further studies on single crystals are highly recommended to establish whether the partial moment freezing is generic to the system (e.g., because of the proximity of the Kitaev QSL to the magnetic ordered phase) or a matter of sample quality (presence of structural disorder). Nonetheless, the study presented here clearly shows that Li_2RhO_3 is not a conventional bulk spin-glass material, the SRO effects are wiped out in magnetic fields, and most importantly, the low-T spin dynamics as well as the specific heat is reminiscent of that of a quantum spin liquid.

[1] L. Balents, Nature **464**, 199 (2010), and references therein.

[2] S. Sachdev, Nat. Phys. **4**, 173 (2008).

[3] C. Lacroix, P. Mendels, and F. Mila, *Introduction to Frustrated Magnetism*, Springer Series in Solid-State Sciences (Springer, New York, 2011), Vol. 164.

[4] J. T. Kheli and W. A. Goddard III, Proc. Natl. Acad. Sci. USA **90**, 9959 (1993).

[5] S.-S. Lee, P. A. Lee, and T. Senthil, Phys. Rev. Lett. **98**, 067006 (2007).

[6] T. Itou, A. Oyamada, S. Maegawa, and R. Kato, Nat. Phys. **6**, 673 (2010).

[7] M. Mourigal, M. Enderle, A. Klöpperpieper, J.-S. Caux, A. Stunault, and H. M. Rønnow, Nat. Phys. **9**, 435 (2013).

[8] J. Nasu, J. Knolle, D. L. Kovrizhin, Y. Motome, and R. Moessner, Nat. Phys. **12**, 912 (2016).

[9] T.-H. Han, J. S. Helton, S. Chu, D. G. Nocera, J. A. Rodriguez-Rivera, C. Broholm, and Y. S. Lee, Nature **492**, 406 (2012).

[10] Y. Shen, Y.-D. Li, H. Wo, Y. Li, S. Shen, B. Pan, Q. Wang, H. C. Walker, P. Steffens, M. Boehm, Y. Hao, D. L. Quintero-Castro, L. W. Harriger, M. D. Frontzek, L. Hao, S. Meng, Q. Zhang, G. Chen, and J. Zhao, Nature **540**, 559 (2016).

[11] M. J. P. Gingras and J. E. Greedan, Rev. Mod. Phys. **82**, 53 (2010).

[12] B. Normand and Z. Nussinov, Phys. Rev. B **93**, 115122 (2016).

[13] A. H. Castro Neto, F. Guinea, N. M. R. Peres, K. S. Novoselov, and A. K. Geim, Rev. Mod. Phys. **81**, 109 (2009).

[14] B. Dora and F. Simon, Phys. Rev. Lett. **102**, 197602 (2009).

[15] Z. Y. Meng, T. C. Lang, S. Wessel, F. F. Assaad, and A. Muramatsu, Nature **464**, 847 (2010).

[16] J. Knolle, D. L. Kovrizhin, J. T. Chalker, and R. Moessner, Phys. Rev. Lett. **112**, 207203 (2014).

[17] J. Knolle, D. L. Kovrizhin, J. T. Chalker, and R. Moessner, Phys. Rev. B **92**, 115127 (2015).

[18] J. Yoshitake, J. Nasu, and Y. Motome, Phys. Rev. Lett. **117**, 157203 (2016).

[19] X.-Y. Song, Y.-Z. You, and L. Balents, Phys. Rev. Lett. **117**, 037209 (2016).

[20] J. Knolle, *Dynamics of a Quantum Spin Liquid,* Springer Theses (Springer International, New York, 2016).

[21] J. Chaloupka, G. Jackeli, and G. Khaliullin, Phys. Rev. Lett. **105**, 027204 (2010).

[22] A. Y. Kitaev, Ann. Phys. (NY) **321**, 2 (2006).

[23] S. Trebst, arXiv:1701.07056.

[24] D. Gotfryd, J. Rusnačko, K. Wohlfeld, G. Jackeli, J. Chaloupka, and A. M. Oles, Phys. Rev. B **95**, 024426 (2017).

[25] S. C. Williams, R. D. Johnson, F. Freund, S. Choi, A. Jesche, I. Kimchi, S. Manni, A. Bombardi, P. Manuel, P. Gegenwart, and R. Coldea, Phys. Rev. B **93**, 195158 (2016).

[26] A. Banerjee, C. A. Bridges, J.-Q. Yan, A. A. Aczel, L. Li, M. B. Stone, G. E. Granroth, M. D. Lumsden, Y. Yiu, J. Knolle, S. Bhattacharjee, D. L. Kovrizhin, R. Moessner, D. A. Tennant, D. G. Mandrus, and S. E. Nagler, Nat. Mater. **15**, 733 (2016).

[27] S.-H. Baek, S.-H. Do, K.-Y. Choi, Y. S. Kwon, A. U. B. Wolter, S. Nishimoto, J. van den Brink, and B. Büchner, Phys. Rev. Lett. **119**, 037201 (2017).

[28] S. H Chun, J.-W. Kim, J. Kim, H. Zheng, C. C. Stoumpos, C. D. Malliakas, J. F. Mitchell, K. Mehlawat, Y. Singh, Y. Choi, T. Gog, A. Al-Zein, M. M. Sala, M. Krisch, J. Chaloupka, G. Jackeli, G. Khaliullin, and B. J. Kim, Nat. Phys. **11**, 462 (2015).

[29] M. Hermanns, S. Trebst, and A. Rosch, Phys. Rev. Lett. **115**, 177205 (2015).

[30] S. K. Choi, R. Coldea, A. N. Kolmogorov, T. Lancaster, I. I. Mazin, S. J. Blundell, P. G. Radaelli, Y. Singh, P. Gegenwart, K. R. Choi, S.-W. Cheong, P. J. Baker, C. Stock, and J. Taylor, Phys. Rev. Lett. **108**, 127204 (2012).

[31] J. Reuther, R. Thomale, and S. Rachel, Phys. Rev. B **90**, 100405(R) (2014).

[32] M. Majumder, M. Schmidt, H. Rosner, A. A. Tsirlin, H. Yasuoka, and M. Baenitz, Phys. Rev. B **91**, 180401(R) (2015).

[33] T. Takayama, A. Kato, R. Dinnebier, J. Nuss, H. Kono, L. S. I. Veiga, G. Fabbris, D. Haskel, and H. Takagi, Phys. Rev. Lett. **114**, 077202 (2015).

[34] S. Manni, Y. Tokiwa, and P. Gegenwart, Phys. Rev. B **89**, 241102(R) (2014).

[35] S. Manni, S. Choi, I. I. Mazin, R. Coldea, M. Altmeyer, H. O. Jeschke, R. Valentí, and P. Gegenwart, Phys. Rev. B **89**, 245113 (2014).

[36] M. Hermanns and S. Trebst, Phys. Rev. B **89**, 235102 (2014).

[37] I. I. Mazin, S. Manni, K. Foyevtsova, H. O. Jeschke, P. Gegenwart, and R. Valentí, Phys. Rev. B **88**, 035115 (2013).

[38] Y. Luo, C. Cao, B. Si, Y. Li, J. Bao, H. Guo, X. Yang, C. Shen, C. Feng, J. Dai, G. Cao, and Z.-a. Xu, Phys. Rev. B **87**, 161121(R) (2013).

[39] See Supplemental Material at http://link.aps.org/supplemental/10.1103/PhysRevB.96.094432 for ac susceptibility results and further details of the analysis of spin lattice relaxation rates, which includes Ref. [40].

[40] F. L. Pratt, Physica B **289-290**, 710 (2000).

[41] S. Nakatsuji, Y. Nambu, H. Tonomura, O. Sakai, S. Jonas, C. Broholm, H. Tsunetsugu, Y. Qiu, and Y. Maeno, Science **309**, 1697 (2005).

[42] R. H. Colman, F. Bert, D. Boldrin, A. D. Hillier, P. Manuel, P. Mendels, and A. S. Wills, Phys. Rev. B **83**, 180416(R) (2011).

[43] J. A. Quilliam, F. Bert, R. H. Colman, D. Boldrin, A. S. Wills, and P. Mendels, Phys. Rev. B **84**, 180401(R) (2011).

[44] S. Nakatsuji, K. Kuga, K. Kimura, R. Satake, N. Katayama, E. Nishibori, H. Sawa, R. Ishii, M. Hagiwara, F. Bridges, T. U. Ito, W. Higemoto, Y. Karaki, M. Halim, A. A. Nugroho, J. A. Rodriguez-Rivera, M. A. Green, and C. Broholm, Science **336**, 559 (2012).

[45] Y. Okamoto, M. Nohara, H. Aruga-Katori, and H. Takagi, Phys. Rev. Lett. **99**, 137207 (2007).

[46] R. Dally, T. Hogan, A. Amato, H. Luetkens, C. Baines, J. Rodriguez-Rivera, M. J. Graf, and S. D. Wilson, Phys. Rev. Lett. **113**, 247601 (2014).

[47] A. C. Shockley, F. Bert, J.-C. Orain, Y. Okamoto, and P. Mendels, Phys. Rev. Lett. **115**, 047201 (2015).

[48] Y. J. Uemura, A. Keren, K. Kojima, L. P. Le, G. M. Luke, W. D. Wu, Y. Ajiro, T. Asano, Y. Kuriyama, M. Mekata, H. Kikuchi, and K. Kakurai, Phys. Rev. Lett. **73**, 3306 (1994).

[49] H. D. Zhou, E. S. Choi, G. Li, L. Balicas, C. R. Wiebe, Y. Qiu, J. R. D. Copley, and J. S. Gardner, Phys. Rev. Lett. **106**, 147204 (2011).

[50] T. Dey, A. V. Mahajan, P. Khuntia, M. Baenitz, B. Koteswararao, and F. C. Chou, Phys. Rev. B **86**, 140405(R) (2012).

[51] V. Todorova and M. Jansen, Z. Anorg. Allg. Chem. **637**, 37 (2011).

[52] H. E. Stanley, Phys. Rev. **158**, 546 (1967); G. S. Rushbrooke and P. J. Wood, Proc. Phys. Soc. A **68**, 1161 (1955).

[53] Y. Singh and P. Gegenwart, Phys. Rev. B **82**, 064412 (2010).

[54] Y. Singh, S. Manni, J. Reuther, T. Berlijn, R. Thomale, W. Ku, S. Trebst, and P. Gegenwart, Phys. Rev. Lett. **108**, 127203 (2012).

[55] S. Manni, Ph.D. thesis, Georg-August-Universitaet Goettingen (2014).

[56] J. A. Mydosh, *Spin Glasses: An Experimental Introduction* (Taylor and Francis, London, 1993).

[57] J. G. Cheng, G. Li, L. Balicas, J. S. Zhou, J. B. Goodenough, Cenke Xu, and H. D. Zhou, Phys. Rev. Lett. **107**, 197204 (2011).

[58] A. P. Ramirez, B. Hessen, and M. Winklemann, Phys. Rev. Lett. **84**, 2957 (2000).

[59] M. J. Lawler, A. Paramekanti, Y. B. Kim, and L. Balents, Phys. Rev. Lett. **101**, 197202 (2008).

[60] Y. Zhou, P. A. Lee, T.-K. Ng, and F.-C. Zhang, Phys. Rev. Lett. **101**, 197201 (2008).

[61] T. K. Dey, A. V. Mahajan, R. Kumar, B. Koteswararao, F. C. Chou, A. A. Omrani, and H. M. Ronnow, Phys. Rev. B **88**, 134425 (2013).

[62] V. M. Katukuri, S. Nishimoto, I. Rousochatzakis, H. Stoll, J. van den Brink, and L. Hozoi, Sci. Rep. **5**, 14718 (2015).

[63] Y. Shimizu, K. Miyagawa, K. Kanoda, M. Maesato, and G. Saito, Phys. Rev. Lett. **91**, 107001 (2003).

[64] Y. Yamada and A. Sakata, J. Phys. Soc. Jpn. **55**, 1751 (1986).

[65] T. Moriya, *Spin Fluctuations in Itinerant Electron Magnetism* (Springer, Berlin, 1985).

[66] N. Bloembergen, E. M. Purcell, and R. V. Pound, Nature **160**, 475 (1947).

[67] A. Abragam, *Principles of Nuclear Magnetism* (Oxford University Press, New York, 1983).

[68] T. Imai, E. A. Nytko, B. M. Bartlett, M. P. Shores, and D. G. Nocera, Phys. Rev. Lett. **100**, 077203 (2008).

[69] P. Mendels and F. Bert, J. Phys. Soc. Jpn. **79**, 011001 (2010).

[70] S. J. Blundell, Contemp. Phys. **40**, 175 (1999); Chem. Rev. **104**, 5717 (2004); A. Yaouanc and P. Dalmas de Réotier, *Muon Spin Rotation, Relaxation, and Resonance* (Oxford University Press, Oxford, UK, 2010).